HIGH SPEED IMAGES OF RESISTANCE SPOT WELDING SYNCHRONIZED WITH ELECTRICAL SIGNALS

José Enrique Vargas
MSc candidate at University of Brasilia (Graco) and Federal University of Uberlândia (Laprosolda).
jevargas@hotmail.com

Marco Antonio Wolff
Undergraduate student, Federal University of Uberlândia, Laprosolda, Campus Santa Mônica, Bloco 1M, 38400-032
mawolff@mecanica.ufu.br

Sadek C. Absi Alfaro
Ph.D. Full Professor, University of Brasilia, Graco, Campus Darcy Ribeiro, 70910-900
sadek@unb.br

Louriel Oliveira Vilarinho
Ph.D. Associate Professor, Federal University of Uberlândia, Laprosolda, Campus Santa Mônica, Bloco 1M, 38400-032
vilarinho@mecanica.ufu.br

Abstract. *Resistance Spot Welding (RSW) is largely used in the automotive industry. It has high production rates (over 30 spots/minute) and good quality. However, the introduction of galvanized plates on production lines brought difficulties on the welding parameters setup. This work aims to present operational envelopes for diferents galvanized plates, wich are further studied by using high speed camera synchronized to the current and voltage signals. The material melting and the weld pool (nugget) are observed and correlated to the electrical signals.*

Keywords*: Resistance Spot Welding, Nugget Formation, High-Speed Filming.*

1. Introduction

The Resistance Spot Welding (RSW) process is one of the most employed manufacturing processes in the automotive industry. In this process, metal sheets are joined by the accomplishment of welded spots from the localized melting due to heat generated by the material resistance of current passage (Joule effect, given by the product of current and resistance: I^2R). The material sheet used by the automotive industry is the mild steel and in the last years the galvanized steel has been employed for cost reduction. Both hot-immersion and electrolytic galvanization have been used. This industrial innovation has brought some complications for the process quality what demanded new research lines.

The scientific literature has focused on the analysis, monitoring and improvement of the mechanisms for the weld lens formation under different conditions, parameters and materials with the objective of welding process optimization. Dickinson et al. (1980) and Kaiser, et al. (1982), among others, tried to understand the effects of the welding parameters on the formation and growth of the lens in an attempt of better controlling these parameters for process optimization. Recently, Cho & Rhee (2003) carried out a study by using a high-speed camera for monitoring the lens growth and its relationship with the process parameters. These authors made used of truncated electrodes (described in Section 2).

Accordingly to this presented research trend, it is aimed here to study the mechanism of the weld lens formation by using high-speed visualization and, differently from other authors, keeping the same level of energy and synchronize with the electrical signals (current and voltage). Three configurations of sheet thickness were employed (namely A, B and C). A practical and technological database was found and the operational envelopes are presented.

2. Experimental Procedure

The welding was made by a spot welding machine composed by a transformer (manufacturer Soltronic HT75 2 MF, 440 V, 75 kVA, 170 A in the primary circuit) and a controller (manufacturer Fase Saldatura with maximum nominal power of 54 kVA) was used to supply a water-cooled electrodes with pneumatic pressure from 87 to 261 kgf, with the welding current (secondary circuit) varying from 2 to 6 kA and maximum welding cycle of 100.

The welding pool visualization was carried out by using a digital high-speed camera (manufacturer Nac, model Memrecam CI V-145-J) set with F-mount lens (Nikon 90 mm, f#2.5 and 55 mm of diameter plus an UV lens). The illumination was made by a light source (model Arrilite 1000, with 1000 w, 60 Hz, 45º-250ºC) in the spot mode (not in the flood mode). A rate of 1000 fps and a shutter time of 1/6000 s were set. The experimental rig is shown in Fig. 1. It must be pointed out that the images are synchronized to the electrical signals by using the procedure described in Bálsamo et al. (2000).

The electrodes (caps) are 16-mm external diameter, spherical type, Class A, Group 2, hardness of 75 HRb and 75% IACS. They were truncated in a 3 mm of length and placed parallel to the sheet as shown in Fig. 2a. This approach is necessary because if truncation is not made, the electrode tend to squeeze the spot. It also promotes a better visualization of the lens formation.

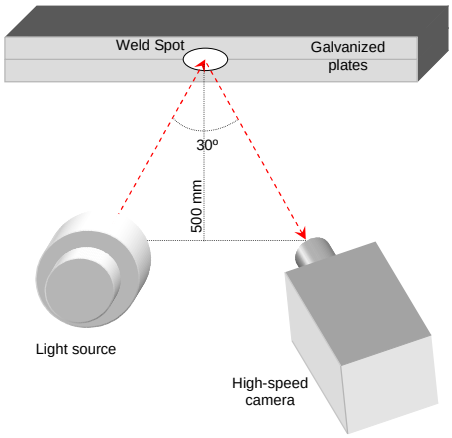

Figure 1. Experimental rig for high-speed filming.

Since the final spot is not welded under a real situation, it must be done a comparison between a real situation and this approach for lens visualization, which is represented in Fig. 2b. This comparison must be performed under two criteria: same energy and same pressure levels. The same energy level is reached by applying Eq. 1 that represents the heat generation by the Joule effect. Considering that the area in the visualization case is half of the one in a real spot welding ($A_2 = A_1/2$), by applying Eq. 1 one finds that the current of the visualization case must be $I_2 = I_1/\sqrt{2}$. In the case of the electrode force (Fel), considering that the pressure upon the spots must remain the same and since the area becomes half of it, then the force should be half of the one in the first case ($F_2 = F_1/2$)

$$E = I_{rms}^2 \cdot R \cdot T_s = I_{rms}^2 \cdot \frac{\rho \cdot \ell}{A} \cdot T_s \tag{1}$$

where, E is the heat generated by the Joule effect in the sheets; I_{rms} is the true rms welding current; R is the sheet resistance; ρ is the sheet electrical resistivity; ℓ is the total sheet thickness; A is the spot area and T_s is the total welding cycle.

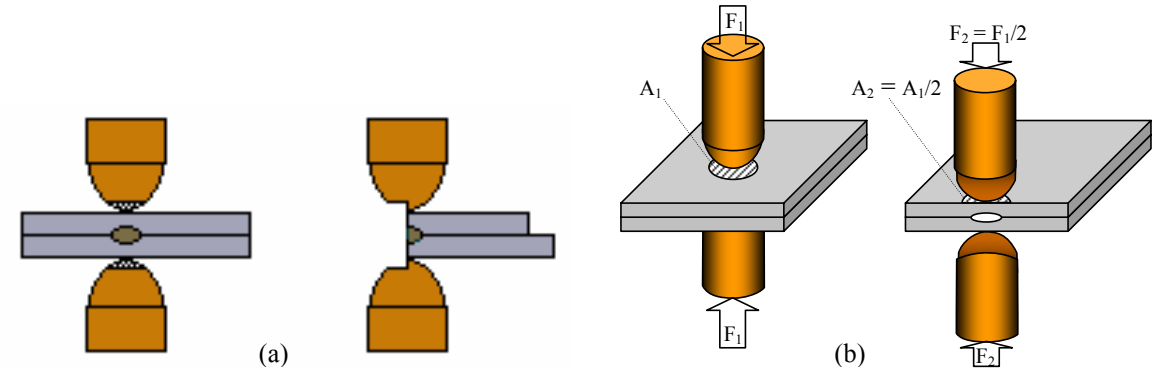

Figure 2. (a) Sheets and caps location for welding procedure and (b) Geometrical aspects of comparing a real situation and the visualization one.

The metal sheets are galvanized ones (hot-immersion technique) and they are clamped together and the spot welding is carried out in the center of one side in order to guarantee repeatability. All sheets have dimension of 100 x 25 mm. Three different configurations are employed, namely A, B and C. Configuration A makes use of sheet thickness of 2.0 and 2.0 mm; configuration B uses sheets of 2.0 and 1.2 mm of thickness, whereas Configuration C employs sheet thickness of 1.2 and 1.2 mm. These sheets were sheared, deburred, aligned and isolated (from each other by a piece of paper in of the ends) in order to avoid shunt effects. The surfaces were cleaned up by detergent and dried in high-pressured air.

The welding procedure was carried out in two stages. The first one aimed to achieve a technological database for industrial application. Thus, operational envelopes were found. These envelopes characterize operational ranges varying from minimum values of current, force and cycles, where the joint is not accomplished, to maximum values where neither material expulsion nor deep depression (indentation) is observed. The second stage comes from the obtained operational envelopes, where five conditions were then selected for visualization of the lens formation. The transposition from the welding conditions obtained from the operational envelopes (real situation) to the visualization case is made by applying the procedure described for Eq. 1.

3. Results and discussion

The obtained operational envelopes are shown in Fig. 3. A total of six envelopes are presented for the three employed configuration of galvanized sheets; one brings rms current (I_{rms}) versus electrode force (Fel) curves and other rms current (I_{rms}) versus total welding cycle (Ts). In the first curves, a constant time of 30 cycles were employed, whereas the second curves, electrode force of 174 kgf were set. These two values were arbitrarily select and represent a situation where a good spot is obtained for the three sheets configurations. It must be pointed out that the electrical frequency is 60 Hz, i.e., the duration of one cycle is equal to 1/60 s.

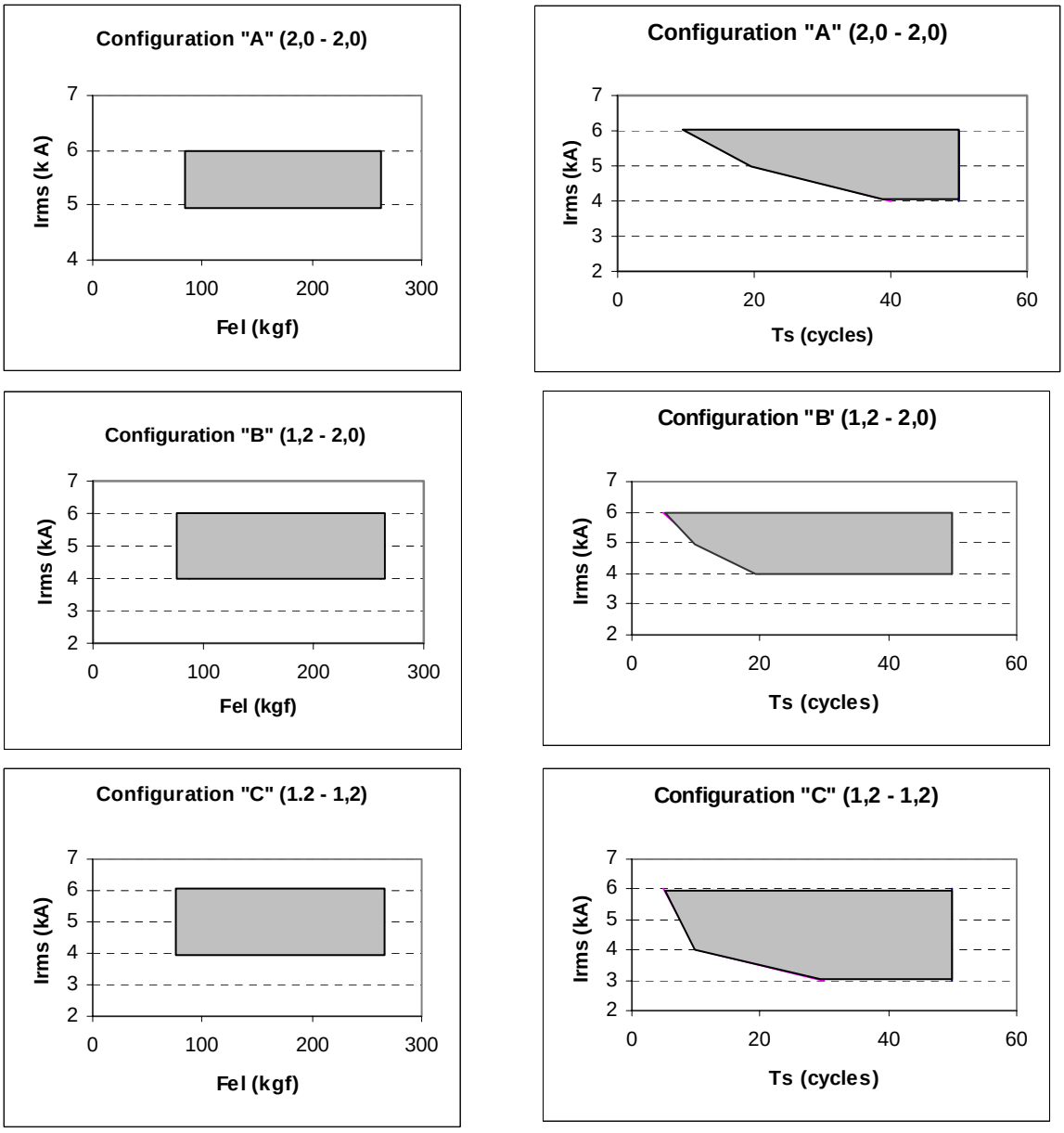

Figure 3. Operational envelopes for both current x force (left) and current x total welding cycle (right).

From these six operational envelopes, five welding conditions were picked up to be characterized. They are shown in Tab. 1. Runs 4735, 4736 and 4737 represent the average central position of the envelopes, i.e., 5 kA; 174 kgf and 30 cycles. As explained in Section 2, these values cannot be promptly used and must be respectively translated to 3.5 kA; 87 kgf and 30 cycles. Runs 4739 and 4740 were made in order to trace a comparison with Run 4735 for investigating the effect of the rms current on the lens formation.

Table 1. Five selected conditions from the operation envelopes. The rms voltage (V_{rms}) was measured by the DAQ system. All runs are for 30 cycles and 87 kgf.

Run	I_{rms} [A]	V_{rms} [V]	Plates Configuration
4735	3504	1,06	A
4736	3534	0,90	B
4737	3561	0,81	C
4739	2060	0,73	A
4740	3027	1,01	A

In Run 4735 (Fig. 4), the first image (frame from down to up) shows the galvanized plates under the electrode force, but without current passing through. The second frame brings the image after the first welding cycle, where liquid drops can be observed forming on the surfaces of the upper sheet. It indicates that the zinc coating started to burn out. In the third frame (10^{th} welding cycle), the number of droplets is high in the area between the two sheet (large volume of zinc coating) and they become to be expelled. Also, the Joule heating starts to turn the sheet reddish and to form the lens. In the fourth frame (12^{th} cycle) these aspects are more pronounced. In the fifth frame (16^{th} cycle), there is no longer coating on the sheet surface and the metal has already started melting. The heat transfer (generation and sinking) between two welding cycles is characterized by frames 6 and seven at the 21^{st} cycle. Although it is small, the hot areas (red area) in these two images are not the same (by digital image processing this aspect can be better visualized and enhanced). After the current pulse the area is larger (6^{th} frame) than after the non-active current time (7^{th} frame). This indicates that the weld pool pulses accordingly to the cycle pulses. A small indentation can also be seen in frames 6 and 7. At the end of the 30^{th} cycle (8^{th} frame), the lens reaches its maximum diameter and it solidify at the 10^{th} frame, after 207 ms that the current stops. The 9^{th} frame is presented for further comparison with Run 4740. At this time (134 ms after cycle ceasing), the lens is still hot and if the electrode force cannot were taken out, defects in the lens would appear.

In Run 4736 (Fig. 4), frames 1 and 2 are similar to the one in Run 4735. In the third frame (10^{th} cycle), the lens starts forming in the thicker plate (higher electrical resistance). At this point the coating has already burned out, because here there is less material to be heated up than in the Run 4735. The squeezing of the thinner plate is also observed. These facts are also observed in the fourth frame (12^{th} cycle). In the fifth frame (16^{th} cycle) the union between the two sheets starts and the lens formation is observed. Similarly to Run 4735, in frames 6 and 7 the size variation of the lens is observed, as well. In the 8^{th} frame (end of the welding time), the lens reaches its maximum size, whereas in frame 9 (after 123 ms of the cycling ceasing) the lens is solidified and the electrode force can be taken out.

In Run 4737 (Fig. 5), frames 1 and 2 can be compared to those from Runs 4735 and 4736, already discussed. In the third and fourth frames (6^{th} cycle), the explosion and expulsion of a droplet from the coating is observed between the two sheets. From the fifth frame (10^{th} cycle) to the seventh one (16^{th} cycle) the lens is formed. Similarly to discussed for Runs 4735 and 4736, a variation of the lens size is verified in images 8 and 9 (21^{st} cycle). The maximum lens size is shown in frame 10 (after the 30^{th} cycle) and the solidification if obtained after 93 ms.

Run 4739 (Fig. 5) uses a lower current than the one in Run 4735 (Tab. 1). In the images a smaller coating burning is observed than if compared to the one in Run 4735. In the third frames color changing can be observed, but without lens formation. This is also observed in frames 4, 5 and 6. The welding cycle ends without the material melting. In frames 7 (after 16 ms of cycle ceasing) and frame 8 (after 256 ms of cycle ceasing), the heat is sunk through the sheets and in frame 6 the sheets are moved away because of the electrode force ceases.

In Run 4740 (Fig. 6), an intermediate current is used if compared to Runs 4735 and 4739. The same events of Run 4735 can also be observed, but in a lower scale. An important observation is the solidification time. As pointed out during the analyses of Run 4735, the lens is completely cooled at 207 ms after the cycle ends, whereas in Run 4740 it happens at 134 ms, because of its lower current level. As a further work, this solidification time can be modeled (analytically or numerically) and the results can be checked by using the present experimental work.

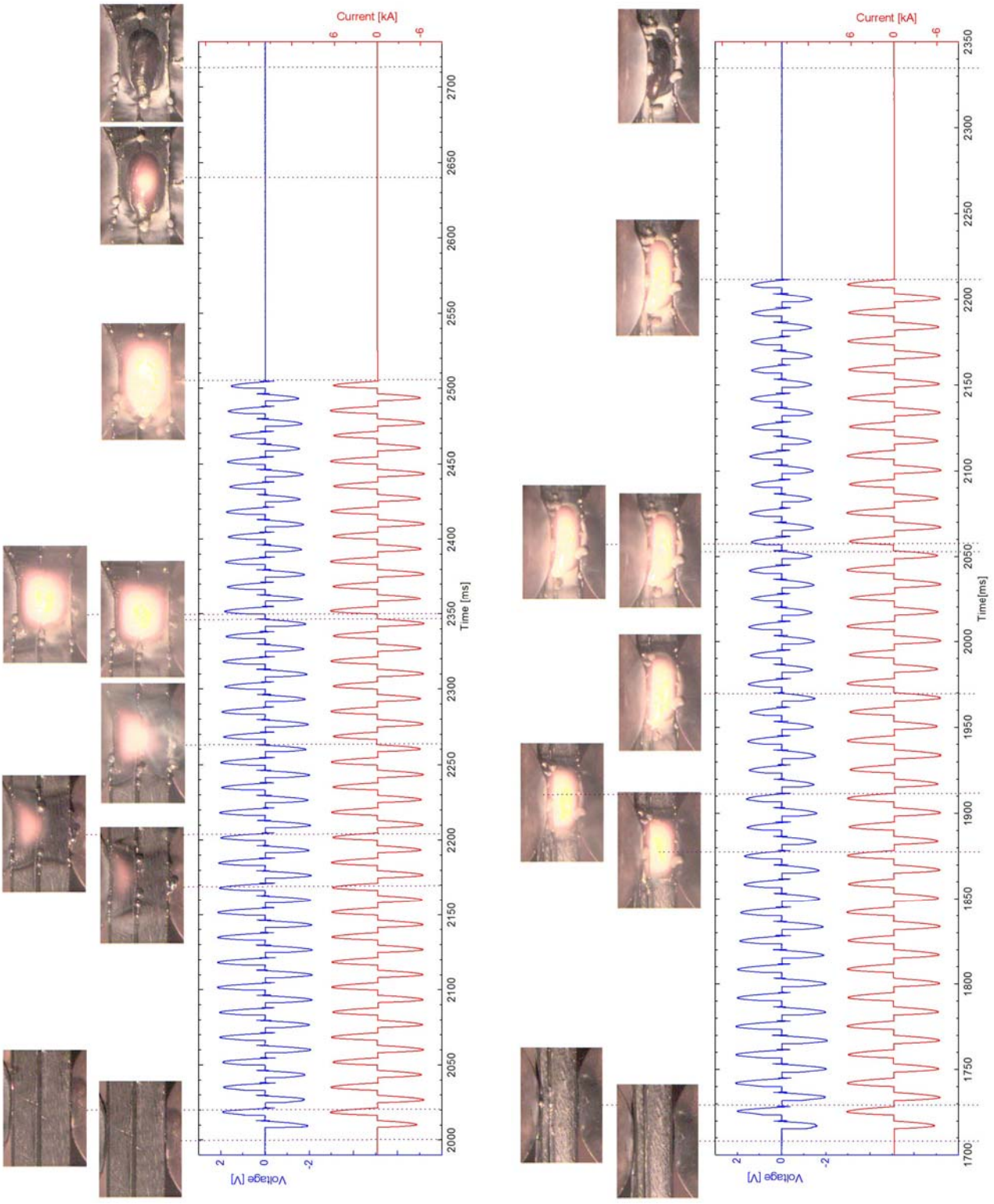

Figure 4 - Synchronized high-speed images with electrical signals for Run 4735 (left) and Run 4736 (right).

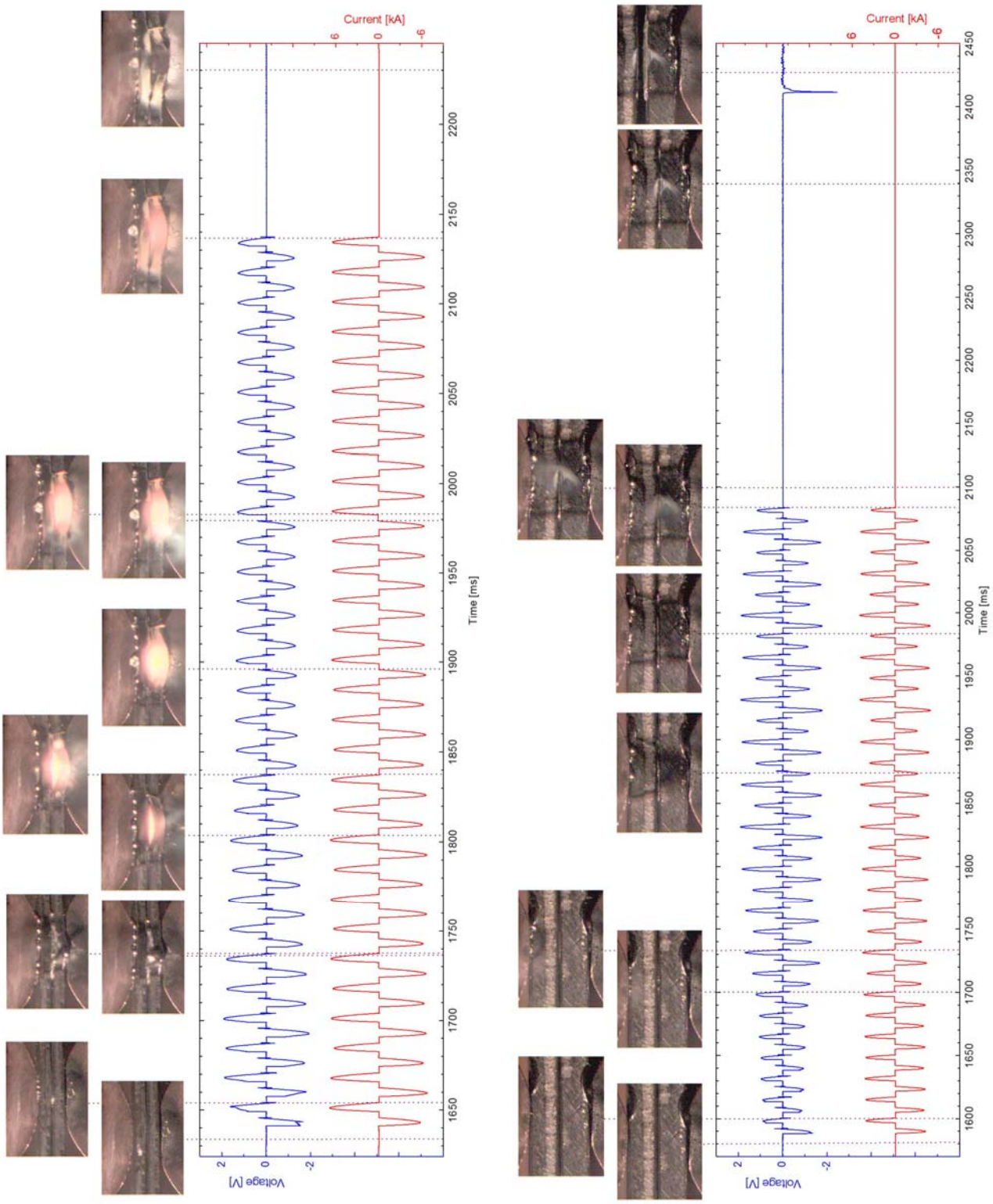

Figure 5 - Synchronized high-speed images with electrical signals for Run 4737(left) and Run 4739 (right).

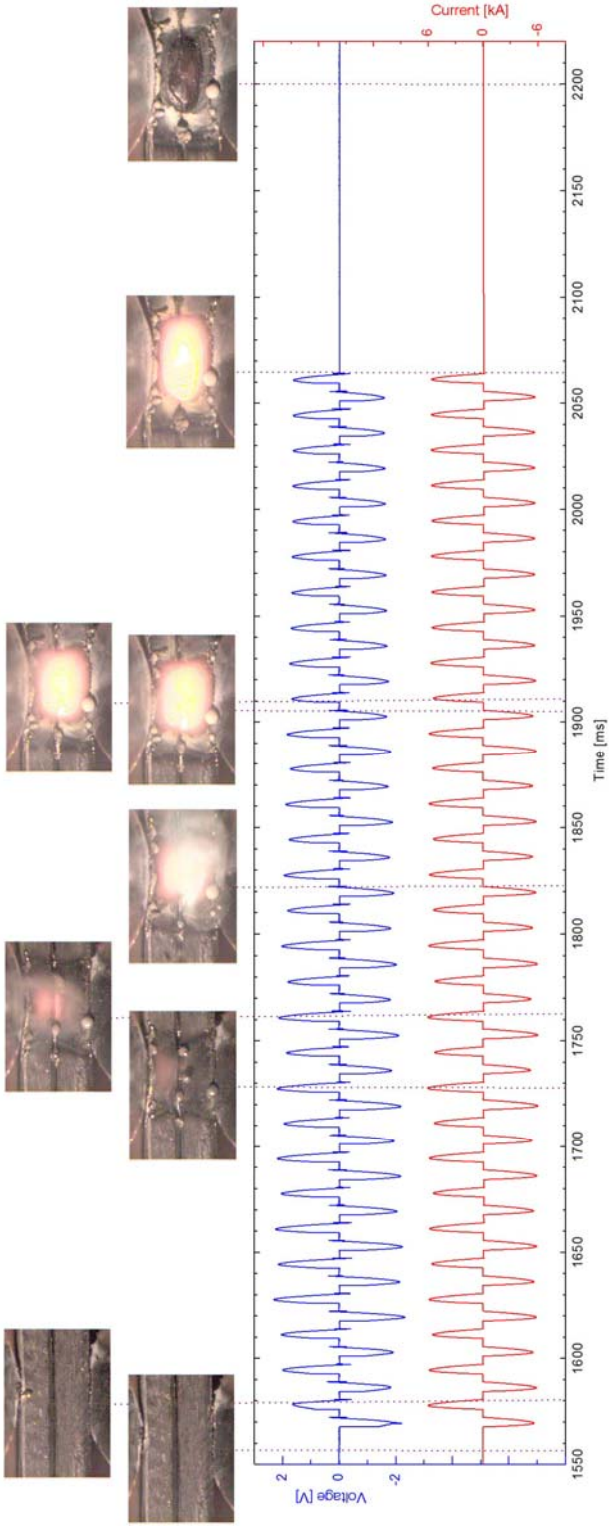

Figure 6 - Synchronized high-speed images with electrical signals for Run 4740.

4. Conclusion

Practical and technological operational envelopes were presented for three different configurations of galvanized sheets jointed by RSW process. Five runs were selected from these envelopes and then the lens formation was visualized by high-speed images. From this procedure and the presented results is possible to conclude that:

- The lens size varies accordingly to the current oscillation (in this case 60 Hz);
- The higher the rms current the longer the solidification time of the lens is required;
- The zinc coating starts to burn out by the first cycle for rms currents above 3 kA;
- Around the 16^{th} cycle the coating no longer exists for rms currents above 3 kA;
- At the 10^{th} welding cycle the lens formation starts to be observed by a reddish area for rms currents above 3 kA;
- For rms currents below 2 kA, no lens was observed.

5. References

Cho, Y., and Rhee, S. 2003, "Experimental Study of Nugget Formation in Resistance Spot Welding". Welding Journal (8): 195-s to 201-s.

Cho, H. S., and Cho, Y. J. 1989. "A study of the thermal behavior in resistace spot welding. Welding Journal 68(6): 236-s to 244-s.

Dickinson, D. W,; Franklin, J. E.; and Stanya, A. 1980. "Characterization of spot welding behavior by dinamic electrical resistance monitoring". Welding Journal 59(6): 170-s to 176-s.

Kayser, J. G., Dunn, G. J., and Eager, T. W. 1982, "The effect of electrical resistance on nugget formation during spot welding. Welding Journal 61(6): 167-s to 174-s

Lane, C. T., Sorensen, C. D., Hunter, G. B., Gedeon, S. A., and Eagar, T.W. 1987. "Cinematography of resistance spot welding of galvanized steel sheet". Welding Journal 66(9): 260-s to 265-s.

Rice, W., and Funk, E. J. 1967. "An analytical investigation of the temperature distributions during restistance welding". Welding Journal 46(4): 175-s to 186-s.

Savage, W. F.; Nippes, E. F.; and Wassell, F. A. 1978. "Dynamic contact resistance of series spot welds". Welding Journal 57(2): 43-s to 50-s.

Sawhill, J. M., Jr., and Baker, J. C. 1980. "Spot weldability of high-strength sheet steels". Welding Journal 59(1): 19-s to 30-s.

Bálsamo, P. S. S., Vilarinho, L. O., M. Vilela, Scotti, A. 2000. "Development of an experimental technique for studying metal transfer in welding: synchronized shadowgraphy". The Int. Journal for the Joining of Materials: v.12, n.2, p.48 - 59.

6. Responsibility notice

The authors are the only responsible for the printed material included in this paper.